

THE ZEEMAN EFFECT AND  $\Lambda$ -TYPE AND SPIN DOUBLING  
IN THE CaH BANDSBY WILLIAM W. WATSON  
SLOANE PHYSICS LABORATORY, YALE UNIVERSITY

(Received November 30, 1931)

## ABSTRACT

A more detailed discussion of the Zeeman effect in the 6389A  ${}^2\Sigma, {}^2\Sigma$  band of CaH than that given previously with W. Bender is presented. General agreement with the assumption that the magnetic energy in a  ${}^2\Sigma$  state is largely due to the interaction of the electron spin and the external field is obtained for band lines of low  $K$  value, but marked differences and asymmetries in the patterns occur for lines from the higher rotational levels. The neglected coupling between the component  $\rho$  of  $L$  along the rotational axis of the molecule and the field will account completely for these deviations, and these observations together with those on the Zeeman effect of the lines of these higher rotational levels in the  ${}^2\Pi, {}^2\Sigma$  band of CaH are shown to be in accord with the explanation by Van Vleck and Mulliken and Christy of the large  $\Lambda$ -type and spin doubling in these states.

## INTRODUCTION

IN A recent paper the writer and W. Bender<sup>1</sup> reported some of the more interesting details of the Zeeman effect in the  ${}^2\Pi, {}^2\Sigma$  band at 7000A and the  ${}^2\Sigma, {}^2\Sigma$  band at 6389A in the spectrum of CaH. It was shown that in the case of the  ${}^2\Pi, {}^2\Sigma$  band the observed Zeeman patterns for lines representing low rotational levels were in substantial agreement with the predictions of Hill's theoretical formulas for the Zeeman effect in  ${}^2\Pi$  states.<sup>2</sup> Marked departures from the predicted patterns for the lines of high  $K$  values were noted, however, and a brief description was given of certain peculiar features of the patterns for the lines of the  ${}^2\Sigma, {}^2\Sigma$  band. In explanation, attention was called to the fact that the very large spin and  $\Lambda$ -type doubling exhibited by the CaH states involved in the production of these bands indicated a relatively large component of the electronic orbital angular momentum perpendicular to the internuclear axis, the coupling of which with the external field could well account for the observed Zeeman patterns. The objects of the present paper are to present a more thorough investigation of the details of the Zeeman effect in the  ${}^2\Sigma, {}^2\Sigma$  band in comparison with theoretical expectations, and to discuss these findings and the corresponding effect in the  $\Pi^2, {}^2\Sigma$  band in relation to new conclusions of Mulliken and Christy<sup>3</sup> concerning the origin of the spin and  $\Lambda$ -type doublings in these bands.

A theoretical treatment by Hill of the action of an external magnetic field on  ${}^2\Sigma$  states has been given by Almy.<sup>4</sup> This treatment considers the mag-

<sup>1</sup> W. W. Watson and W. Bender, Phys. Rev. **35**, 1513 (1930).

<sup>2</sup> E. L. Hill, Phys. Rev. **34**, 1507 (1929).

<sup>3</sup> R. S. Mulliken and A. Christy, Phys. Rev. **38**, 87 (1931).

<sup>4</sup> G. M. Almy, Phys. Rev. **35**, 1495 (1930).

netic energy to be largely due to the interaction between the spin and the field, so that if the spin doubling at the origin of the band is small, the spin is oriented either parallel or anti-parallel to the field. The coupling of the spin with the external field in the molecule is still present, however, and so each member of this twice normal doublet is split into  $2J+1$  magnetic sublevels. With increase of the rotational quantum number  $K$ , the spin doubling may become much larger than  $\Delta 2\nu_n$  in which case the relative orientation of  $S$  and  $K$  remains and these magnetic levels should be spaced in the interval from about  $+\Delta\nu_n$  to  $-\Delta\nu_n$  about the no-field position. Assuming that the perturbation energy is entirely due to the interaction of spin and field, Hill gets the following solution for the energy determinant:

$$W = \pm \frac{1}{2} \{ \nu_0^2 + 4M\nu_0\Delta\nu_n / (K + \frac{1}{2}) + 4\Delta\nu_n^2 \}^{1/2} \quad (1)$$

where  $\nu_0$  is the spin doublet width for the  $K$  level under consideration, the  $+$  sign is for the  $T_1$  levels ( $J = K + \frac{1}{2}$ ), the  $-$  sign for the  $T_2$  levels ( $J = K - \frac{1}{2}$ ), and  $W$  is measured from the center of the no-field doublet. For the two outermost sublevels  $M = \pm (K + \frac{1}{2})$  of the  $J = K + \frac{1}{2}$  states, the energies are given by

$$W = \nu_0/2 \pm \Delta\nu_n. \quad (2)$$

It should be emphasized that in this theory the interaction energy of  $S'$  and  $H$  is just added to the experimentally known  $\nu_0$ , no consideration being given to the origin of the spin doubling<sup>5</sup> and to the possibility of there being a sizable interaction between the component  $\rho$  of  $L$  perpendicular to the internuclear axis in the molecule and the external field. We return to this point below. In combination with Hill's formulas for the Zeeman effect in  ${}^2\Pi$  states, however, this treatment of the effect in  ${}^2\Sigma$  states has already been shown to supply a good agreement up to moderately large  $K$  values with the observed patterns in  ${}^2\Pi$ ,  ${}^2\Sigma$  bands of  $\text{OH}^4$  and  $\text{ZnH}$  and  $\text{CdH}$ .<sup>6</sup>

The nature of the spin and  $\Lambda$ -type doubling in these electronic states has been made more evident by the recent work of Mulliken and Christy,<sup>3</sup> who use these  $\text{CaH}$  bands as one example showing the excellent agreement with Van Vleck's theoretical equations. These equations for the energy all involve terms responsible for the doubling which contain factors of the form  $|BL_y(\Pi, \Sigma^+)|^2 / \nu(\Pi, \Sigma)$ , where the  $L_y$  is one of the components  $L_x$  and  $L_y$  of the electronic orbital angular momentum vector  $L$  perpendicular to the electric axis, and the  $\nu(\Pi, \Sigma)$  is the frequency of any  $\Pi \rightarrow \Sigma$  transition from the  $\Pi$  state in question to any  $\Sigma$  state and  $\nu$  value. From the numerical values and signs of the  $p_0$  and  $q_0$  for the doubling in this  ${}^2\Pi$  state of  $\text{CaH}$ , and the equality of this  $p_0$  with the  $\gamma_0$  of the spin doubling of the upper  ${}^2\Sigma$  state,<sup>7</sup> it is to be concluded that these two states stand in a relation of "pure precession" with each other. That is, these two states of the  $\text{CaH}$  molecule share the same  $l$ , and differ only in that  $\Lambda = 1$  for the  ${}^2\Pi$  state and  $\Lambda = 0$  for the  ${}^2\Sigma$ . The calculated  $p_0$ ,  $q_0$  and  $\gamma_0$ , assuming pure precession, agree well with the observed constants al-

<sup>5</sup> J. H. Van Vleck, Phys. Rev. **33**, 467 (1929).

<sup>6</sup> W. W. Watson, Phys. Rev. **36**, 1134 (1930).

<sup>7</sup> Cf. details given in reference 3.

though the  $|\nu(\Pi, \Sigma)|$  is only  $1320 \text{ cm}^{-1}$ . And since from the value of the coupling constant  $A$ , as well as from other evidence, the  ${}^2\Pi$  state is no doubt  $\dots 4p\pi$ , this upper  ${}^2\Sigma$  must be  $\dots 4p\sigma$  and not  $3d\sigma$  as earlier assumed by Mulliken.

The spin doubling  $\Delta\nu_{12}(K)$  in the upper  ${}^2\Sigma$  state becomes exceptionally large, as compared to that in most known  ${}^2\Sigma$  states,<sup>8</sup> it being  $-22 \text{ cm}^{-1}$  at  $K=33$ . For the same  $K$  in the  ${}^2\Pi_d$  state, the spin doubling equals  $+20 \text{ cm}^{-1}$ . Now as Mulliken and Christy point out,<sup>9</sup> these  $\Delta\nu_{12}$  quantities may be expected to be equal to  $A\rho$ , where  $A$  is the same coupling constant as holds for the interaction of  $S$  and  $\Lambda$  in the  ${}^2\Pi$  state. This  $A=80$ , and so it is to be concluded that the  $\rho$ , which is the component of  $l$  along the direction of  $K$ , is about 0.25. This represents a large uncoupling, and yet the Van Vleck formulas agree remarkably well with the data. These  ${}^2\Sigma, {}^2\Sigma$  bands represent, then, a good opportunity for the study of the Zeeman effect for such transitions. The formulas of Hill given above serve as a guide in the measurement and interpretation of the observed patterns, and it is evident that any marked departures from the predicted patterns are to be attributed to the neglected possibility of coupling between the  $\rho$  and the field.

#### EXPERIMENTAL PROCEDURE AND CALCULATIONS

The spectrograms showing the Zeeman effect in the 6389A  ${}^2\Sigma, {}^2\Sigma, (0, 0)$  band of CaH measured in this investigation were mostly those produced with W. Bender,<sup>1</sup> but some more plates were also taken at several field strengths to verify the conclusions. The technique of the production of the spectrograms was the same as previously described. For the sake of brevity only measurements at two strengths of field before considered—14,000 and 24,600 gauss—will be described, with brief reference to some further changes in the patterns exhibited at the highest field strength—29,950 gauss.

Computation of the magnetic levels according to Eqs. (1) and (2) for both of the  ${}^2\Sigma$  levels has been made for each field strength. The value of  $\nu_0$  for the ground state has been taken to be  $0.045(K + \frac{1}{2})$ , while for the upper state computation of the doublet interval for each value of  $K$  has been made from the original analysis of Hulthén.<sup>10</sup> The solid lines in Fig. 1 give the course of these levels for increasing  $K$  for  $H=24,600$  gauss, only the extreme values of  $M = \pm J$  and  $M=0$  being shown. From such a diagram, giving consideration to the proper change in  $K$  for the band lines in question, and to the selection rule  $\Delta M = 0$  and  $\pm 1$ , the predicted Zeeman patterns can be computed. Transitions from the  $T_1'$  levels to the  $T_1''$  levels and from the  $T_2'$  levels to the  $T_2''$  levels give the narrow "outside" blocks of Zeeman components, while the cross-over transitions for the  $T_1'$  group of levels to the  $T_2''$  group and from the  $T_2'$  group to the  $T_1''$  group are responsible for the broad "inside" blocks of components outlined in Fig. 2 and 3. To be noted is the predicted symmetry of the pat-

<sup>8</sup> The writer and W. Fredrickson have recently reported (Abstract, Chicago meeting Am. Phys. Soc., Nov. 1931) a considerably larger and similar doubling in a corresponding  ${}^2\Sigma$  state of SrH.

<sup>9</sup> Reference 3, p. 118.

<sup>10</sup> E. Hulthén, Phys. Rev. **29**, 97 (1927).

terns of the corresponding lines in the  $P_1$  and  $P_2$  or  $R_1$  and  $R_2$  branches, because of the equality in the over-all width of the levels in the  $T_1$  and  $T_2$  groups.

One can get some idea of the correction that must be applied to these computed widths of the groups of levels, due to the presence of the interaction between the component  $\rho$  of  $l$  in the direction of  $K$  and the external field  $H$ , by assuming that the magnetic moment associated with  $\rho$  is that fraction of a Bohr magneton that  $\rho$  is of unit component of  $l$ .<sup>11</sup> Some values of  $\rho$  for this upper  $^2\Sigma$  state, estimated from the spin doublet widths as indicated above for  $K = 32$ , together with their product with  $\Delta\nu_n$  for the two field strengths, are given in Table I. This additional magnetic energy for the extreme components  $M = \pm J$  should be either added to or subtracted from that due to the

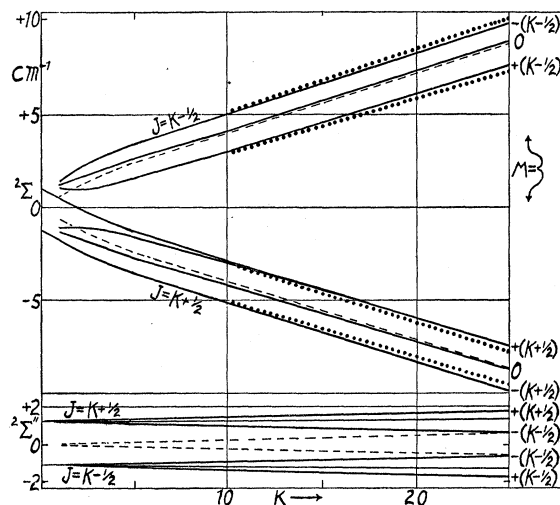


Fig. 1. Magnetic energy level diagram for 6389A  $^2\Sigma$ ,  $^2\Sigma$  band of CaH. Dashed lines give the spacing of the levels without the external field. The solid lines represent the levels for the extreme values of  $M$  and for  $M=0$ , the other values of  $M$  falling fairly uniformly in between. These levels are calculated with equations 1 and 2, with observed spin doubling separations, and therefore assume the magnetic energy to arise only from the interaction of electron spin and field. The dotted lines give the positions of the extreme levels when the additional energy due to the interaction of the component  $\rho$  of  $l$  along the rotational axis and the field is included.

TABLE I. Some values of  $\rho$  for upper  $^2\Sigma$  state, and corresponding magnetic energy for the two strengths of field.  $\text{cm}^{-1}$  units.

$K$	$\rho (= \Delta\nu_{12} \cdot A)$	$H = 14,000$ gauss $\rho \times \Delta\nu_n$	$H = 24,600$ gauss $\rho \times \Delta\nu_n$
10	0.10	0.07	0.12
15	0.14	0.09	0.16
20	0.18	0.12	0.21
25	0.22	0.15	0.26

interaction of  $S$  and  $H$ . That it should be subtracted, not added, is demonstrated by the agreement of the resulting pattern widths with the observa-

<sup>11</sup> I am indebted to R. S. Mulliken for this suggestion.

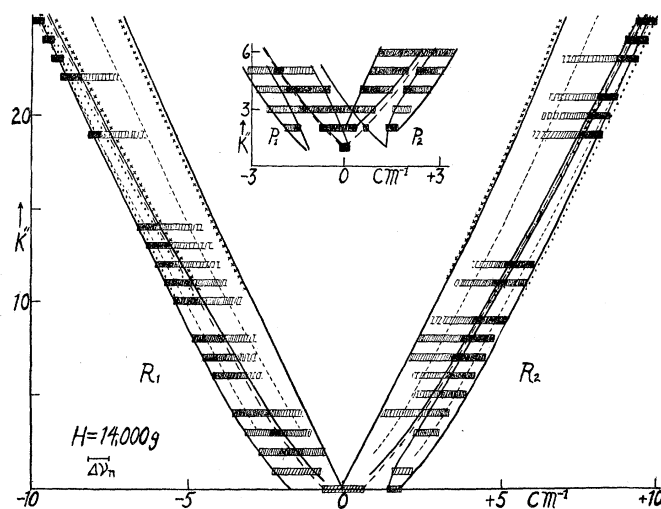


Fig. 2. Comparison of observed and calculated Zeeman patterns for  $H=14,000$  gauss. Heavy dashed lines give no-field positions of the band lines, solid lines give the outlines of the blocks assuming the coupling of the electron spin and the field  $H$  to be the only magnetic energy, and the thin dashed lines the transitions  $M'=0$  to  $M''=0$ . Corrected widths of pattern blocks for higher  $K$  levels upon inclusion of the energy of interaction of the component  $\rho$  of  $l$  along the rotational axis and  $H$  are indicated by the dotted lines for the narrow outside blocks and by the small crosses for the wide inside blocks. The shaded strips at each  $K''$  level give the observed patterns, with the strength of the shading proportional roughly to the intensity. Note the general agreement with the computed patterns for the lines of low  $K$  values, and the evidence for the corrected widths at the highest  $K$  levels.

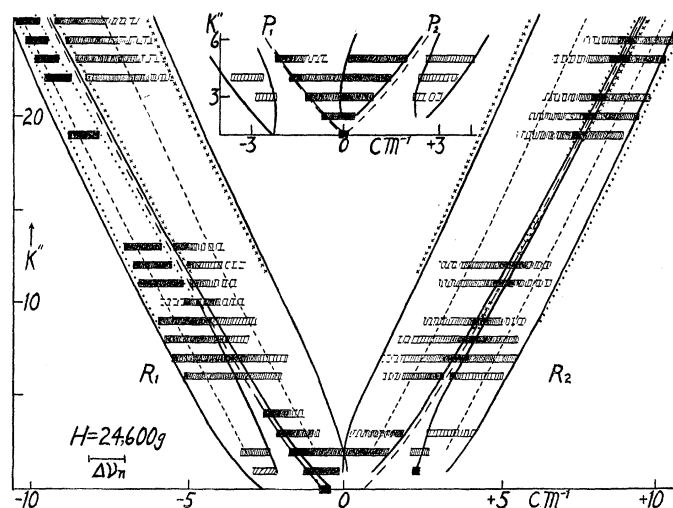


Fig. 3. Comparison of observed and calculated Zeeman patterns for  $H=24,600$  gauss. Note the greater intensity of the inner blocks of components for lines of low  $K''$  values, the evidence for the corrected widths of the patterns at the higher  $K$  levels (narrow  $R_1$ -blocks and intensity of  $R_2$  patterns around no-field position), and the setting-in of these effects at lower  $K$  levels ( $K''=11$ ) than in Fig. 2.

tions. That is, for the  $J = K + \frac{1}{2}$  group of levels, the magnetic energy for  $M = \pm J$  is  $\pm [\Delta\nu_n \text{ (for the } S) - \rho \times \Delta\nu_n]$ , while for the  $J = K - \frac{1}{2}$  group it is  $\pm [-\Delta\nu_n \text{ (for the } S) - \rho \times \Delta\nu_n]$ . This reduces the over-all width of the magnetic levels for the  $T_1$  group by  $2 \times \rho \times \Delta\nu_n$ , and increases the width for the  $T_2$  group by the same amount. And since for this  ${}^2\Sigma$  state the  $l$ -uncoupling is very appreciable, there results the considerable correction to the widths of the groups of Zeeman levels indicated by the dotted lines in Fig. 1. The fact that this additional magnetic energy must be subtracted from that for the  $S$  and  $H$  interaction means that the  $\rho$  must be oriented anti-parallel to  $K$  along the rotational axis of the molecule. Finally, this quantity  $\rho$  is very small for the lower  ${}^2\Sigma$  state for these bands, and should therefore have a negligible effect on the Zeeman patterns.

#### DETAILS OF THE ZEEMAN EFFECT IN THE ${}^2\Sigma$ , ${}^2\Sigma$ BAND

The comparison of the observed pattern blocks for the two field strengths is made in Tables II and III and in Figs. 2 and 3. These graphs display the results much more vividly than do the tables, and so the attempt is made to represent as much of the information as possible in this form. Because of the fact that the  $P_1$  and  $P_2$  branches rather rapidly converge to form the heads of the band, the patterns of these lines overlap each other too much for  $K > 6$  to make measurement possible. The patterns are better resolved in the  $R$  branches, but even for these the patterns cannot be measured for quite a number of the lines due to the proximity of either another main  $R$  line or of a line of the (1, 1) band.

The positions of the no-field band lines are given by the heavy dashed curves of Figs. 2 and 3, while the outlines of the Zeeman pattern blocks of unresolved components are indicated by the solid lines for the calculations which include only the interaction of  $S$  and  $H$ . Corrected pattern widths resulting from the inclusion of the appreciable interaction energy of  $\rho$  and  $H$  for the higher  $K$  levels are indicated by the dotted lines for the outside, narrower blocks and by the lines of small crosses for the inside, broader blocks. The somewhat narrower blocks on the high frequency (+) side of the  $R_2$  and  $P_2$  lines and on the low frequency (-) side of the  $R_1$  and  $P_1$  lines are due respectively to the transitions from the  $J = K - \frac{1}{2}$  group of levels of the  ${}^2\Sigma'$  state to the  $J = K - \frac{1}{2}$  group of levels in the  ${}^2\Sigma''$  state in Fig. 1 and from the  $J = K + \frac{1}{2}$  group of  ${}^2\Sigma'$  to the  $J = K + \frac{1}{2}$  group of  ${}^2\Sigma''$ . The rather broader "inside" blocks for these lines arise from the cross-over transitions from the  $J = K - \frac{1}{2}$  group of levels of the upper state to the  $J = K + \frac{1}{2}$  group of the lower state and from the  $J = K + \frac{1}{2}$  group of the upper state to the  $J = K - \frac{1}{2}$  group of the lower state respectively. In no instance are separate components of the Zeeman patterns resolved, although for  $P_1(1\frac{1}{2})$  and  $R_1(\frac{1}{2})$  a number of superposed components of zero displacement give rise to a sharp line in the field exposure. At each  $K$  level in Figs. 2 and 3 the shaded block gives the extent of the observed pattern and the relative intensities are represented by the density of the shading. In Fig. 4 enlargements of portions of the spectrograms at the two field strengths are presented in order to give an indication of the character of the observed patterns.

TABLE II. Comparison of some observed and predicted pattern blocks for  $R$  lines of low  $K$  values in  $\text{CaH } ^2\Sigma, ^2\Sigma$  band. Magnetic energy only that of interaction of spin and field. (+ = displacement to high frequency, - = to low frequency from no-field position.  $\text{cm}^{-1}$  units.)

$K$	$R_1$		$H = 14,000$ gauss		$R_2$	
	Calc.	Obs.	Calc.	Obs.	Calc.	Obs.
1	-0.41 to -1.06; 0; +0.18 to +0.64 and +0.93	-1.00 to about +0.53	+0.41 to +1.12 and -0.22 to -0.95		+0.43 to +1.02 weak	
3	-1.04 to 0 and +0.10 to +1.20	-1.06 through stronger 0 to weak +edge	+0.20 to +1.06 and +0.11 to -1.24		+ edge at +0.92	
4	0 to -1.03 and +0.09 to +1.35	0 to -1.02 stronger, and 0 to about +1.20 weak	+0.14 to +1.02 and -0.11 to -1.35		+ edge at +0.82, weak at 0 and weak—block to indef. edge	
7	0 to -0.93 and +0.07 to +1.53	0 to -0.87 strong	+0.10 to +0.92 and -0.08 and -1.53		+ edge at +0.89, stronger at 0 and weaker to -1.54	
11	0 to -0.77 and +0.06 to +1.76	-0.11 to -0.77 strong, and -0.11 to beyond +1.11 weak	+0.07 to +0.79 and -0.07 to -1.76		+edge at +0.72, stronger at 0 and weaker—to indef. edge	
$H = 24,600$ gauss						
1	-2.06; -1.78 to -1.02; 0; +0.24 to +0.86; +1.29	-1.00 to indef.-edge weak; 0 to about +1.00 strong	+1.04 to +2.07 and -0.28 to -1.34		+1.04 sharp; no other +; —block obscured	
2	-0.73 to -2.08; 0; +0.15 to +1.69	-0.74 to -1.62 weak; + strong 0 to $R_2$ —block	+0.82 to +2.09 and -0.20 to -1.55		+0.38 to +0.99; — strong fusing with $R_1$ +block	
3	-0.56 to -2.07; 0; +0.14 to +1.90	+ block strong 0 to weaker fusion with $R_2$ —	+0.58 to +2.03 and -0.22 to -1.87		+0.55 to ? weak; — strong but fused with other	
7	0 to -1.95 and +0.19 to +2.45	stronger 0 to +1.89; +0 to (weaker) indef. edge	+0.23 to +1.91 and -0.17 to -2.43		0 strong; + to +1.89; — block same intensity	
11	0 to -1.78 and +0.16 to +2.75	-0.19 to -1.64 strong; +0 stronger, gradually fading out	+0.14 to +1.79 and -0.11 to -2.71		strong center +0.04 to -0.16; + and — both gradually fade out	

TABLE III. Comparison of some observed and predicted pattern blocks for  $R$  lines of high  $K$  values in  $\text{CaH } ^2\Sigma, ^2\Sigma$  band. Magnetic interaction energy includes that of  $\rho$  (component of  $l$  along rotational axis) and field.

$K$	$R_1$		$H = 14,000$ gauss		$R_2$	
	Calc.	Obs.	Calc.	Obs.	Calc.	Obs.
19	-0.12 to -0.37 and +0.15 to +2.04	-0.22 to -0.63 strong; +very weak to indef. edge	-0.07 to +0.61 and +0.04 to -2.27		-0.10 to +0.68 strong; — very weak to indef. edge	
22	-0.14 to -0.26 and +0.16 to +2.14	-0.12 to -0.54 strong; + block very weak	-0.08 to +0.51 and +0.06 to -2.41			
23	-0.15 to -0.26 and +0.17 to +2.18	-0.16 to -0.57 strong	-0.10 to +0.50 and +0.09 to -2.49		-0.10 to +0.58; — too weak to measure	
24	-0.15 to -0.24 and +0.17 to +2.22	-0.16 to -0.52 strong	-0.10 to +0.46 and +0.09 to -2.54		-0.11 to +0.56 strong	
25	-0.15 to -0.24 and +0.17 to +2.27	-0.14 to -0.53 strong	-0.11 to +0.43 and +0.11 to -2.59		-0.13 to +0.56 strong	
$H = 24,600$ gauss						
19	-0.21 to -1.28 and +0.31 to +2.89	-0.29 to -1.23 strong; + fused with another	-0.14 to +1.70 and +0.15 to -3.32		center very strong +0.12 to -0.32; + edge +1.35; — weaker to indef. edge	
22	-0.24 to -1.11 and +0.33 to +3.21	-0.20 to -1.04 strong; + broad +0.20 to indef. edge	-0.18 to +1.60 and +0.18 to -3.49			
23	-0.25 to -1.05 and +0.33 to +3.05	-0.30 to -1.07 strong; +0.18 to indef. edge broad	-0.20 to +1.56 and +0.19 to -3.55		center stronger +0.30 to -0.38; + block strong to +1.44; — is weak	
24	-0.26 to -1.00 and +0.34 to +3.08	-0.34 to -1.04 strong; +0.20 to indef. edge fairly strong	-0.21 to +1.54 and +0.32 to -3.60		center stronger +0.20 to -0.43; + strong to +1.43; — edge very weak	
25	-0.27 to -0.98 and +0.34 to +3.12	-0.32 to -1.06 strong; + begins quite strong at +0.21	-0.22 to +1.50 and +0.22 to -3.67			

There is good agreement in general for the lower rotational levels up to  $K'' = 14$  at  $H = 14,000$  gauss and to  $K'' = 9$  at  $H = 24,600$  gauss between the observed Zeeman patterns and those predicted on the assumption that the

magnetic energy is very largely that of spin and field. A few points here deserve special mention. For  $P_1(1\frac{1}{2})$  only a single sharp undisplaced component (six possible  $M' \rightarrow M''$  transitions) is observed at all field strengths, with no

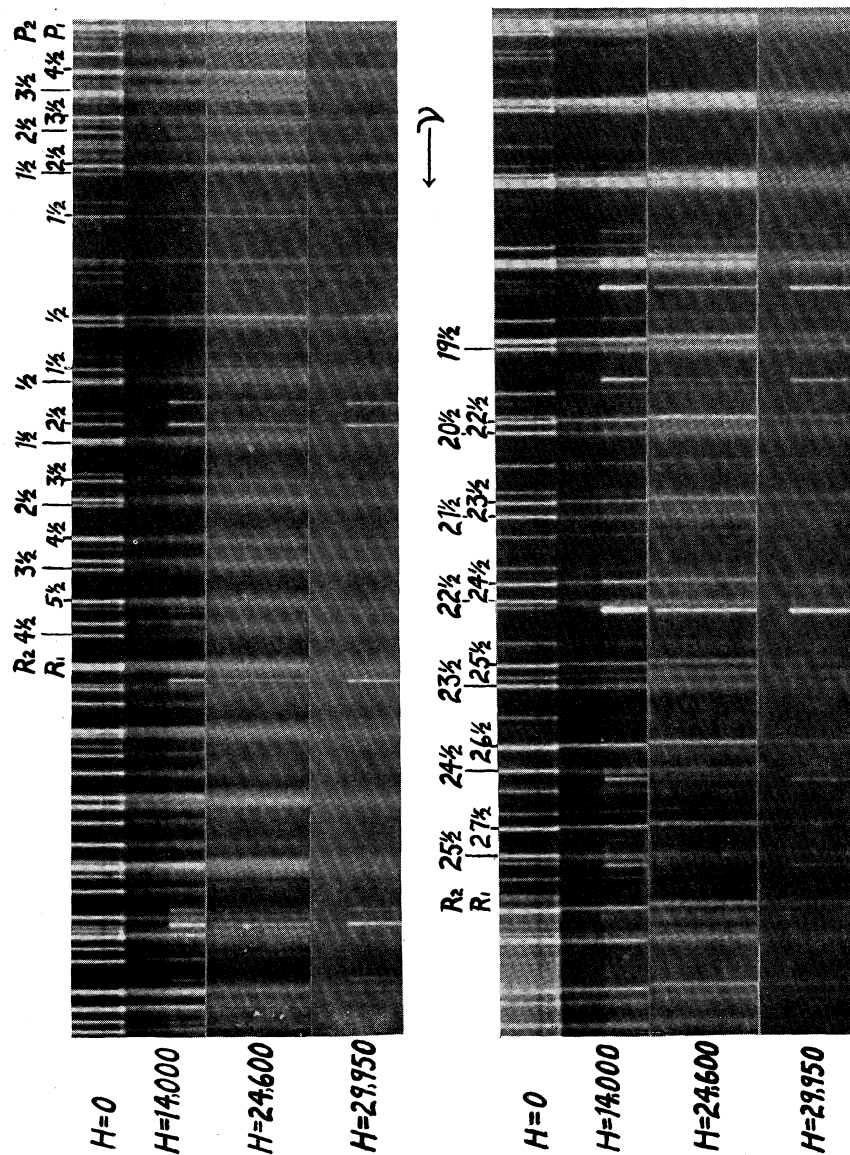


Fig. 4. Enlargements of portions of the spectrograms showing the Zeeman effect in the 6389  $^2\Sigma, ^2\Sigma$  band of CaH. The shorter lines in the field exposures are the Fe comparison spectrum.

trace of the possible "wings" (two components each) at about  $+\Delta\nu_n$  and  $-\Delta\nu_n$ . At the lower field strength for the lowest  $K$  values the two blocks of compo-



nents are of about equal intensity, but with increasing  $K$  the outside ( $-$ ) blocks of the  $R_1$  lines become narrower and stronger, while the accompanying broader inside ( $+$ ) blocks become weaker and fade out to an indefinite outer edge. In the corresponding  $R_2$  line patterns the same is true, with the greatest intensity, however, at the no-field positions. For  $H = 24,600$  gauss the inside ( $+$ ) blocks for the  $R_1$  and  $P_1$  lines and ( $-$ ) blocks for the  $R_2$  and  $P_2$  lines with  $K'' < 6$  are considerably the stronger, and for  $H = 29,950$  gauss these are the only components visible, the patterns now filling entirely the no-field interval between the two components of the spin doublet, but with the edges of the blocks nearest the no-field positions the most intense.

This change in the patterns for the lines of low  $K$  value indicates the action of a molecular Paschen-Back effect, for with high field strength the interval between the two components of these spin doublets is of the order of  $2\Delta\nu_n$ .  $S$  then tends to be quantized separately in the field, and the operation of the selection rule  $\Delta M_s = 0$  would cause the observed limitation of the patterns to the inside blocks with the near edges stronger. For  $K'' > 6$  even the highest field is no longer "strong," so that the outer blocks appear and gain in strength as  $K$  increases.

For the  $R$  lines representing the higher rotational levels these outer blocks, the  $+$  blocks for the  $R_2$  lines and the  $-$  blocks for the  $R_1$  lines predominate. But, as Figs. 2 and 3 show, these blocks are neither found to be bounded by the predicted pattern outlines assuming the magnetic energy to be only that of the interaction of  $S$  and  $H$  (the solid black lines), nor do they preserve the indicated symmetry between the  $R_1$  and  $R_2$  patterns. Rather are these patterns found to agree very well with the predictions which also include the magnetic energy due to the coupling of  $\rho$  and the external field  $H$ , represented in Figs. 2 and 3 by the dotted lines for the more intense outside blocks and by the lines of small crosses for the broad, weak, inside blocks for both the  $R_1$  and  $R_2$  lines. The near edge of the narrow intense  $R_1$  blocks for  $K'' > 22$  at  $H = 14,000$  gauss coincides nicely for each band line with the predicted interval from the no-field position. The observation that these  $R_1$  blocks extend out farther to the low frequency side than predicted is no doubt due to the concentration of most of the components at this outer edge, owing to the fact that the  $M' = M'' = 0$  line actually falls outside the limits for the extreme transitions. In the  $R_2$  branch the corresponding pattern blocks are observed to be much broader, and coincide almost exactly with the confines set by the corrected theory.

The data for  $H = 24,600$  gauss offer even more convincing evidence for the inclusion of the magnetic energy arising from the  $l$ -uncoupling in this  $^2\Sigma$  state of CaH. For the intense  $-$  block of components for each  $R_1$  line is observed narrowed just the calculated amount, and the inner edge of the broad  $+$  portion of the pattern falls in each case at just about the calculated separation from the no-field position. Incidentally, these  $+$  blocks, though broader, are considerably more intense than at the lower field strength. As for the  $R_2$  line patterns, the corrected theory explains at once the outstanding feature, the greater intensity at and near the no-field positions of the lines. For the

two parts of the pattern are broadened to such an extent by the effect of the energy of interaction of  $\rho$  and  $H$  that they overlap considerably. And as noted in the  $R_1$  line patterns, these broader blocks of components have their greatest intensity always adjacent to the no-field position, for which the transitions involve the magnetic levels having anti-parallel  $S$  and  $H$ . The outermost edges of these very broad blocks are of such low intensity in our spectrograms that they are just lost in the general fog on the plates.

Measurements of the spectrogram taken at  $H = 29,950$  gauss only serve to verify the results at the other two field strengths. The differences between the patterns of the  $R_1$  and  $R_2$  lines are more marked, and agree closely with the calculations of the complete theory.

#### ZEEMAN EFFECT IN THE ${}^2\Pi \rightarrow {}^2\Sigma$ BAND OF CAH

Because of the pure precession relation which exists between this upper  ${}^2\Sigma$  state and the  ${}^2\Pi$  state of the 7000A CaH band, there should be equally prominent effects on the Zeeman patterns of the lines arising from these higher rotational levels in this  ${}^2\Pi \rightarrow {}^2\Sigma$  band because of the  $l$ -uncoupling. But the spin doubling which originates in this way in the  ${}^2\Pi$  state (Mulliken and Christy's  $\Delta\nu_{12}(K) - [HVV, \Delta\nu_{12}(K)]$  differs for the  ${}^2\Pi_d$  and  ${}^2\Pi_e$  levels, being practically identical with the spin doubling in the upper  ${}^2\Sigma$  state for the former and almost negligible for the latter. This means that for the  $Q$  branch lines, which originate in the  $T_e$  sublevels of the  ${}^2\Pi$  state, the Zeeman patterns even for quite large values of  $K$  should be those given by Hill's treatments of the effect in  ${}^2\Pi$  and  ${}^2\Sigma$  states. For the  $P$  and  $R$  branch lines, however, which involve the  ${}^2\Pi_d$  terms, the magnetic energy due to the interaction of the  $\rho$  and the field  $H$  should be considered in calculating the Zeeman patterns. It is clear that the addition of this interaction will cause one of the groups of magnetic levels in the  ${}^2\Pi$  state to be broadened, while the other group is contracted in its over-all width. This should result in marked differences between the patterns of the  $P_1$  and  $P_2$  or  $R_1$  and  $R_2$  band lines, and a considerable discrepancy between the observations on these patterns and the predictions from Hill's formulas.

The data on the Zeeman effect in this  ${}^2\Pi \rightarrow {}^2\Sigma$  band, though incomplete, are in accord with these considerations. The writer and W. Bender<sup>1</sup> have shown that for the band lines near the origin, there is general agreement with the patterns predicted from Hill's theory. Very great differences in the patterns of the  $P_1$  and  $P_2$  lines from the higher rotational levels were observed, however, the field radiation associated with the  $P_1$  lines becoming very broad whereas for the  $P_2$  lines there occurs just a rather narrow and intense inside block of components. No such differences exist between the patterns of the corresponding  $Q_1$  and  $Q_2$  lines, though observation is made difficult by much overlapping of patterns, but there is a considerable difference in the intensity distribution in the  $Q$  patterns as compared with the  $P$  line patterns.

One might make some rough calculations on the widths of these Zeeman levels in the  ${}^2\Pi$  state after the fashion of our treatment above for the upper  ${}^2\Sigma$  state, assuming case  $b$  for the higher rotational levels, but such a calculation

has not been found satisfactory. In this  ${}^2\Pi$  state there is the usual gradual transition from case  $a$  to case  $b$ , as  $K$  increases, and the addition of the perturbing term due to the interaction of  $\rho$  and  $H$  to the rigorous treatment for the no-field situation would be a difficult task. We have shown, however, that this additional magnetic energy is present in the Zeeman effect in these states of CaH, and that with its inclusion in the theory all the details of the Zeeman effect in the  ${}^2\Sigma$ ,  ${}^2\Sigma$  band can be explained particularly well. Moreover these results are in complete agreement with our earlier conclusions, and with the interpretation by Van Vleck and Mulliken and Christy of the  $\Lambda$ -type and spin doubling in these states.

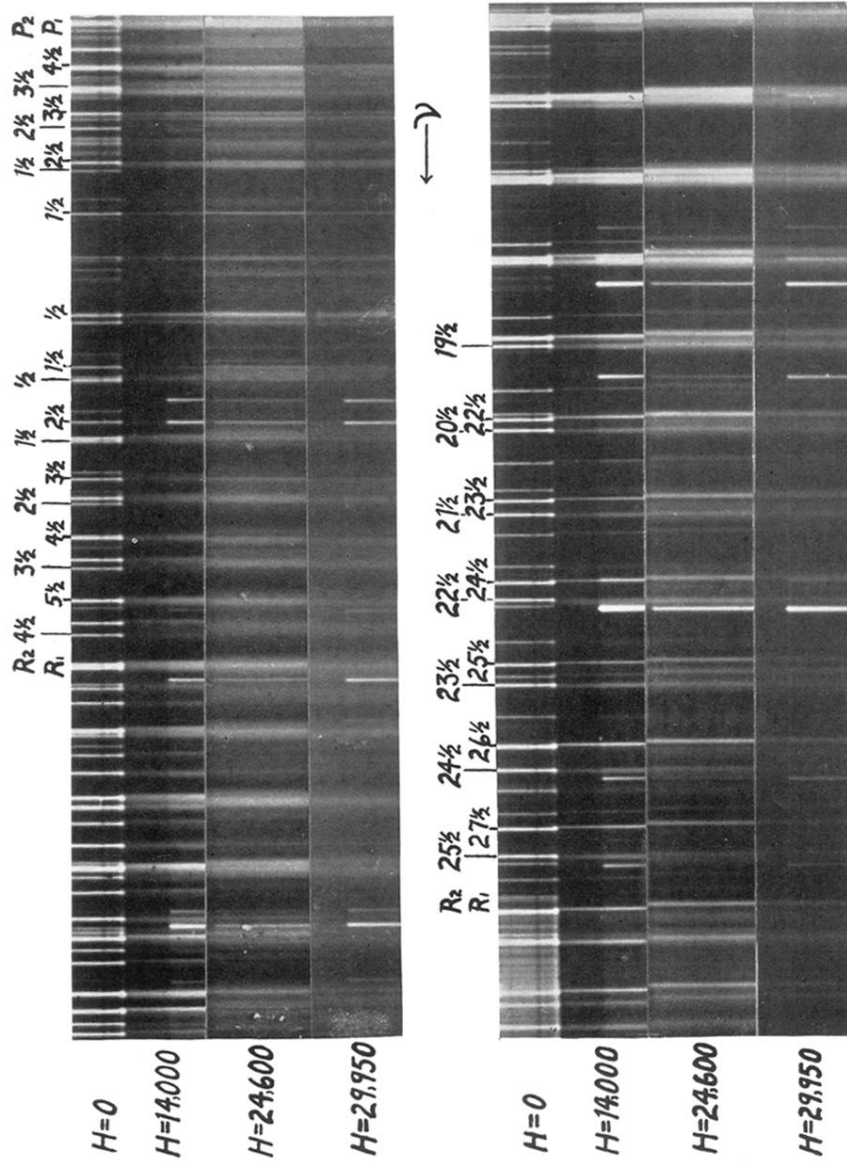


Fig. 4. Enlargements of portions of the spectrograms showing the Zeeman effect in the 6389  ${}^2\Sigma, {}^2\Sigma$  band of CaH. The shorter lines in the field exposures are the Fe comparison spectrum.